Magnetic excitations in the spin-1/2 triangular-lattice antiferromagnet Cs_2CuBr_4

2015 New J. Phys. 17 113059

(http://iopscience.iop.org/1367-2630/17/11/113059)

New Journal of Physics
The open access journal at the forefront of physics

Deutsche Physikalische Gesellschaft DPG
IOP Institute of Physics

Published in partnership with: Deutsche Physikalische Gesellschaft and the Institute of Physics

OPEN ACCESS

RECEIVED
13 August 2015

REVISED
13 October 2015

ACCEPTED FOR PUBLICATION
26 October 2015

PUBLISHED
27 November 2015

PAPER

Magnetic excitations in the spin-1/2 triangular-lattice antiferromagnet Cs_2CuBr_4

S A Zvyagin[1,12], M Ozerov[1,8], D Kamenskyi[1,9], J Wosnitza[1,2], J Krzystek[3], D Yoshizawa[4], M Hagiwara[4], Rongwei Hu[5,6,11], Hyejin Ryu[5,6,12], C Petrovic[5,6] and M E Zhitomirsky[7]

[1] Dresden High Magnetic Field Laboratory (HLD-EMFL), Helmholtz-Zentrum Dresden-Rossendorf, D-01328 Dresden, Germany
[2] Institut für Festkörperphysik, TU Dresden, D-01062 Dresden, Germany
[3] National High Magnetic Field Laboratory, Florida State University, Tallahassee, FL 32310, USA
[4] Center for Advanced High Magnetic Field Science (AHMF), Graduate School of Science, Osaka University, Toyonaka, Osaka 560-0043, Japan
[5] Condensed Matter Physics and Materials Science Department, Brookhaven National Laboratory, Upton, NY 11973, USA
[6] Department of Physics and Astronomy, Stony Brook University, Stony Brook, NY 11794-3800, USA
[7] Service de Physique Statistique, Magnétisme et Supraconductivité, UMR-E9001 CEA-INAC/UJF, F-38054 Grenoble Cedex 9, France
[8] Present address: FELIX Laboratory, Radboud University Nijmegen, 6525 ED Nijmegen, The Netherlands
[9] Present address: High Field Magnet Laboratory (HFML-EMFL), Radboud University Nijmegen, 6525 ED Nijmegen, The Netherlands
[10] Present address: Rutgers Center for Emergent Materials and Department of Physics and Astronomy, Rutgers University, Piscataway, NJ 08854, USA
[11] Present address: Advanced Light Source, EO Lawrence Berkeley National Laboratory, Berkeley, CA 94720, USA
[12] Author to whom any correspondence should be addressed.

E-mail: s.zvyagin@hzdr.de

Keywords: magnetism, frustration, spectroscopy

Abstract

We report on high-field electron spin resonance (ESR) studies of magnetic excitations in the spin-1/2 triangular-lattice antiferromagnet Cs_2CuBr_4. Frequency-field diagrams of ESR excitations are measured for different orientations of magnetic fields up to 25 T. We show that the substantial zero-field energy gap, $\Delta \approx 9.5$ K, observed in the low-temperature excitation spectrum of Cs_2CuBr_4, (Zvyagin *et al* 2014 *Phys. Rev. Lett.* **112** 077206) is present well above T_N. Noticeably, the transition into the long-range magnetically ordered phase does not significantly affect the size of the gap, suggesting that even below T_N the high-energy spin dynamics in Cs_2CuBr_4 is determined by short-range-order spin correlations. The experimental data are compared with results of model spin-wave-theory calculations for spin-1/2 triangular-lattice antiferromagnet.

Spin-1/2 Heisenberg antiferromagnets (AFs) on triangular lattices form an important class of low-dimensional (low-D) spin systems to probe effects of quantum fluctuations, magnetic order, and frustrations. In 1973, developing the idea of the 'resonating valence bond' ground state, Anderson proposed that quantum fluctuations can be sufficiently strong to destroy the classical 120° order in such a system [1]. As consequence, a two-dimensional spin-liquid phase may be realized. This phase can be regarded as a 2D fluid of resonating spin-singlet pairs, with the excitation spectrum formed by fractionalized mobile quasiparticles. Subsequent numerical studies have, however, confirmed the presence of the semiclassical 120° magnetic ordering albeit with strongly reduced ordered moments [2–5]. In recent years, the topic of spin-1/2 Heisenberg AFs on a triangular lattice has received particular attention due to the rich phase diagram, whose details are still actively debated [6–11].

Cs_2CuCl_4 and Cs_2CuBr_4 are two prominent members of this family of frustrated spin systems. Inelastic neutron-scattering experiments in Cs_2CuCl_4 revealed the presence of a highly dispersive continuum of excited states [12]. These excitations were initially identified as spinons in the 2D frustrated spin liquid. Later on, the data have been re-interpreted in the frame of the 1D spin-liquid scenario [13, 14] with interchain bound spinon excitations (triplons) as a signature of the quasi-1D nature of magnetic correlations in this material[13] [15].

[13] We have to mention that in the framework of this interpretation some questions, such as a relatively small spin reduction in the 3D magnetically ordered state $\Delta S/S = 25\%$ [15], remain open.

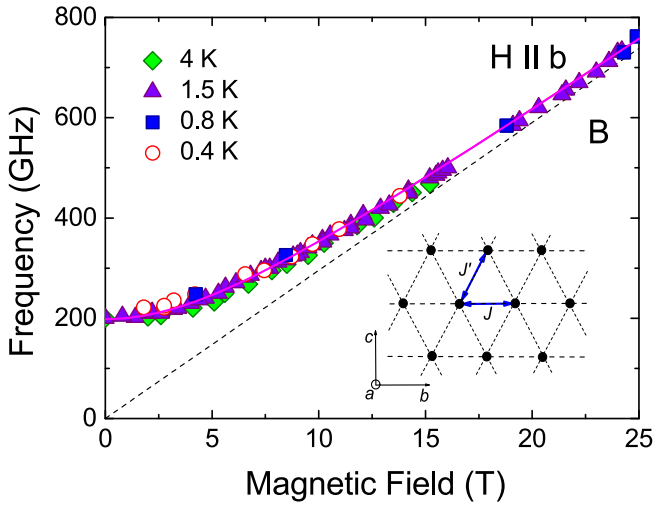

Figure 1. Frequency-field diagram of ESR excitations obtained for Cs_2CuBr_4 with magnetic field applied along the *b*-axis at different temperatures (mode B). Fit results for 1.5 K using equation (1) are shown by the solid line. The frequency-field dependence of the paramagnetic resonance with $g_b = 2.11$ is shown by the dashed line. The inset shows a schematic picture of exchange paths in the *bc*-plane of Cs_2CuBr_4.

Electron spin resonance (ESR) studies provided additional support for the proposed quasi-1D Heisenberg AF chain model with the uniform Dzyaloshinskii–Moriya (DM) interaction, opening an energy gap, $\Delta = 14$ GHz, at the Γ point [16].

Cs_2CuBr_4 realizes a distorted triangular lattice with orthorhombic crystal structure, space group *Pnma*, and the room-temperature lattice parameters $a = 10.195$ Å, $b = 7.965$ Å, and $c = 12.936$ Å ($Z = 4$) [17]. Compared to $J'/J \simeq 0.3$ [18, 19] for Cs_2CuCl_4, the J'/J ratio for Cs_2CuBr_4 is somewhat larger, $J'/J \simeq 0.41$ [18], that places this compound further away from the decoupled AF chain limit and makes it more frustrated. This difference is thought to be related to the 1/3 magnetization plateau and the cascade of field-induced phase transitions, observed in Cs_2CuBr_4 [20, 21]. In spite of intensive theoretical and experimental efforts, very little is known about the spin dynamics in Cs_2CuBr_4. Inelastic neutron-scattering studies have been reported in [22]; unfortunately, due to the limited spectral resolution many important details of the magnetic excitation spectrum appear missing. Nevertheless, ESR experiments on Cs_2CuBr_4 in the fully spin-polarized phase above $H_{sat} \sim 30$ T [18] detected the exchange mode, allowing to estimate parameters of the effective spin Hamiltonian, $J/k_B = 14.9$ K, $J'/k_B = 6.1$ K (where J and J' are the exchange coupling parameters along the horizontal and zigzag bonds, respectively, see figure 1, inset). Besides, the ESR experiments revealed a substantial zero-field gap, $\Delta \approx 200$ GHz, whose nature has so far remained unclear. In this work, we continue high-field ESR studies of Cs_2CuBr_4, evidenced by its remarkable spin dynamics.

Cs_2CuBr_4 single crystals were synthesized by slow evaporation of aqueous solutions of CsBr and $CuBr_2$ similar to the procedure described in [17]. Experiments were done using high-field ESR installations at the Dresden High Magnetic Field Laboratory (HLD, Germany), the Center for Advanced High Magnetic Field Science (Osaka University, Japan), and the National High Magnetic Field Laboratory (Florida State University, Tallahassee, USA) [23]. The experiments were done in the frequency range of 100–800 GHz, using tunable sources of millimeter-wave radiation sources backward wave oscillators (product of ISTOK, Russia), VDI transmit systems (product of Virginia Diodes Inc., USA), and MVNA vector network analyzer (product of AB Millimetre, France).

A single-line ESR absorption was detected in the paramagnetic phase ($T \gg J/k_B$), yielding $g_a = 2.15(2), g_b = 2.07(2), g_c = 2.23(2)$ ($T = 294$ K) and $g_a = 2.15(2), g_b = 2.11(2), g_c = 2.26(2)$ ($T = 77$ K). Pronounced evolution of the ESR spectrum was observed upon cooling.

The frequency-field diagram of magnetic excitations in Cs_2CuBr_4 measured between 0.4 and 4 K for magnetic fields, H, applied along the *b*-axis is shown in figure 1. Some examples of ESR spectra of magnetic excitations at different frequencies are presented in figure 2. For this orientation, a single gapped mode (labeled B) was observed, whose frequency-field dependence can be described using the equation:

$$h\nu = \sqrt{\left(g^*\mu_B H\right)^2 + \Delta^2}, \quad (1)$$

where ν is the resonance frequency, h is the Planck constant, μ_B is the Bohr magneton, g^* is the paramagnetic g factor (the g factor measured at $T = 77$ K, $g^* = 2.11$, was used for the fit and calculations), and Δ is the zero-

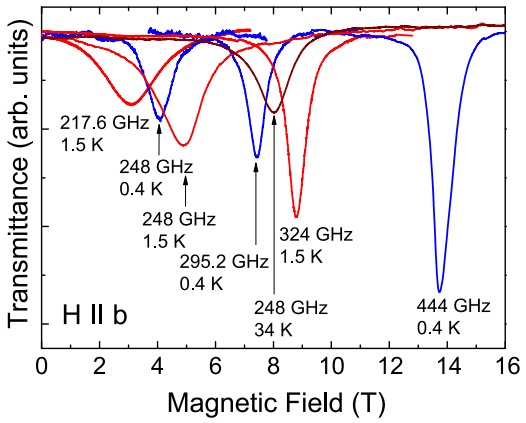

Figure 2. Examples of ESR spectra taken at different frequencies and temperatures with magnetic field applied along the *b*-axis.

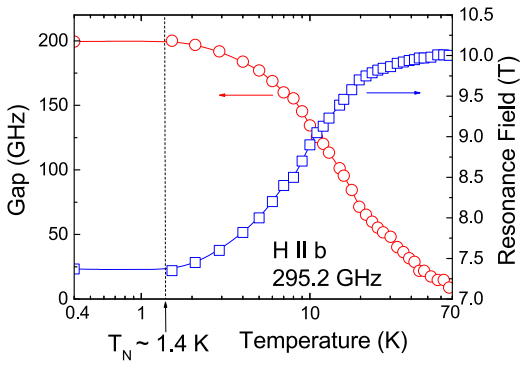

Figure 3. Temperature dependence of the resonance field (squares; the data are taken at 295.2 GHz with magnetic field applied along the *b*-axis) and the zero-field gap size (circles) calculated using equation (1) (see the text for details). Lines are guides for the eye.

field excitation gap. The best fit was obtained using $\Delta = 199(4)$ GHz (which corresponds to 9.5 K) for $T = 1.5$ K.

The temperature dependence of the ESR field position at a frequency of 295.2 GHz with magnetic field applied along the *b*-axis is shown in figure 3 by squares. Using these data and equation (1), the gap size Δ can be calculated for different temperatures (circles in figure 3). We found that the gap in Cs_2CuBr_4 persists up to relatively high temperatures ($T \sim J/k_B$ and above), suggesting the presence of short-range-order spin correlations, responsible for the gap opening, well above T_N.

At $T_N = 1.4$ K Cs_2CuBr_4 undergoes a transition into a 3D long-range ordered phase. Noticeably, the transition leaves the gap size almost unchanged (figure 3). Similar effects were observed in a number of quantum AFs [24–27], whose ground states below T_N are 3D magnetically ordered and the low-energy excitation spectra are determined by 3D long-range-order correlations, while the high-energy ($\sim J$) spin dynamics is still determined by low-D effects. Remarkably, no ESR line-width anomaly was observed in Cs_2CuBr_4 at the transition into the 3D magnetically ordered state (figure 4). The temperature evolution of ESR spectra taken at 295.2 GHz with magnetic field applied along the *b*-axis is shown in figure 5.

Overall, the ESR properties of Cs_2CuBr_4 in many respects appear very similar to those obtained for Cs_2CuCl_4 [16]. On the other hand, contrary to Cs_2CuCl_4 with the zero-field energy gap $\Delta \sim D \approx 0.15J$, the size of the gap in Cs_2CuBr_4 ($\Delta \approx 0.6J$) is too large to be explained in terms of the quasi-1D Heisenberg AF chain model with the uniform DM interaction *D*. This strongly suggests that, compared to Cs_2CuCl_4, the effect of frustrated interactions on the spin dynamics (and more generally, on the magnetic properties) in Cs_2CuBr_4 can be different.

To get an insight into the spin dynamics of Cs_2CuBr_4, we did simple spin-wave calculations for the ordered state of an orthorhombically distorted triangular-lattice antiferromagnet. The minimal spin Hamiltonian includes only exchange interactions

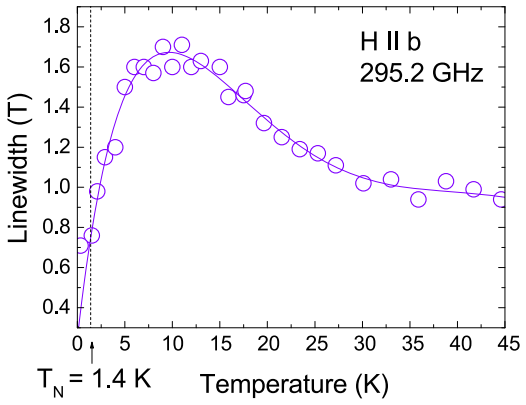

Figure 4. Temperature dependence of the ESR linewidth measured at a frequency of 295.2 GHz with magnetic field applied along the *b*-axis. Line is guide for the eye.

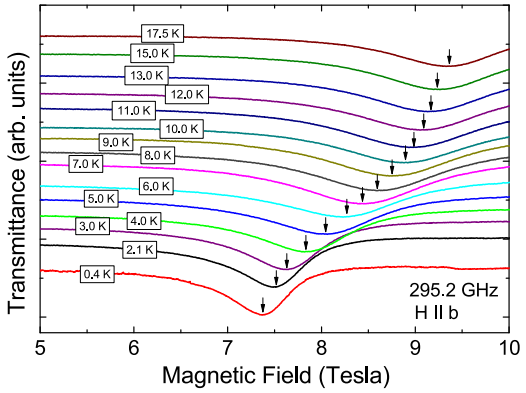

Figure 5. Temperature evolution of ESR spectra taken at 295.2 GHz with magnetic field applied along the *b*-axis (mode B).

$$\hat{\mathcal{H}} = \sum_{\langle ij \rangle} J_{ij}\, \mathbf{S}_i \cdot \mathbf{S}_j, \tag{2}$$

where the nearest-neighbor exchange constant is $J_{ij} = J$ or J' for horizontal or zigzag bonds, respectively[14] (see the inset in figure 1) [28]. The classical ground state of the spin model (2) is a planar spiral magnetic structure with the ordering wave-vector $\mathbf{Q} = (0,\ Q,\ 0)$ and $\cos(Qb/2) = -J'/2J$. At zero temperature, the energy of magnetic excitations in a spiral AF is given by the standard expression [29, 30]:

$$\epsilon_{\mathbf{k}} = S\sqrt{\left(J_{\mathbf{k}} - J_{\mathbf{Q}}\right)\left(\frac{1}{2}J_{\mathbf{k}+\mathbf{Q}} + \frac{1}{2}J_{\mathbf{k}-\mathbf{Q}} - J_{\mathbf{Q}}\right)}, \tag{3}$$

where $J_{\mathbf{k}} = \sum_j J_{ij}\, e^{i\mathbf{k}(\mathbf{r}_i - \mathbf{r}_j)}$ is the Fourier transform of the exchange interactions.

In the framework of the formulated toy model, the origin of the gap may be understood if real geometry of DM interactions in Cs_2CuBr_4 is taken into account [6, 18]. The staggered component of the DM interaction reduces the translational symmetry of the spin Hamiltonian (2) producing a doubling of the unit cell in the *bc* plane and, consequently, folding of the Brillouin zone. As a consequence, an excitation with a momentum $\mathbf{k}$ mixes with another magnon at $\mathbf{k} + q_c^*$, where $\mathbf{q}_c{}^* = (0,\ 0,\ 2\pi/c)$ is a new reciprocal lattice vector. The actual shift of the magnon energy (3) produced by the DM interactions may be quite small because of smalness of D/J. However, the presence of a nonzero mixing matrix element leads to a finite ESR response for the high-energy magnon at the M point ($\mathbf{q}_c{}^*$) in the unfolded Brillouin zone, see figure 6. It is worthwhile to mention that ESR transitions at the Brillouin zone boundary were observed in a number of low-D quantum magnets (see, e.g., [31–34]), while the corresponding selection rules were theoretically studied in [35]. Remarkably, as revealed experimentally [33, 34], such nominally forbidden ESR transitions (which become allowed in the presence of the

[14] It is important to mention that more complex picture of magnetic interactions, including five components of DM interactions (two staggered and three uniform) and a finite interplane interaction need to be taken into account for the accurate quantitative description of the spin dynamics in this compound, in particular, in applied magnetic fields.

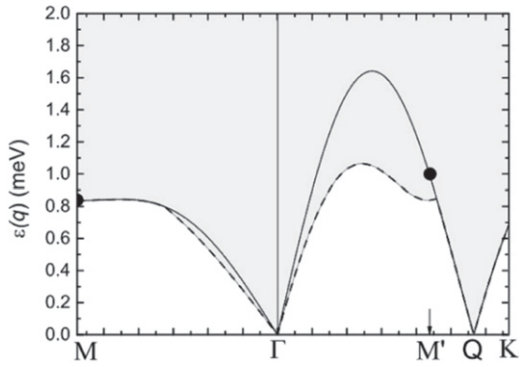

Figure 6. Calculated magnon dispersion in Cs_2CuBr_4. The Γ point refers to the center of the Brillouin zone, whereas Q is the ordering wave vector. The rf field in ESR experiments can excite magnons at points M and M′ due to the staggered DM interaction. The two-magnon continuum is shown in gray color.

DM interaction) can be very intensive, exhibiting, on the other hand, a very pronounced polarization dependence.

The corresponding ESR gap is calculated using equation (3) as

$$\Delta = \epsilon_{\mathbf{q}_c^*} = 4J'S\left(1 - \frac{J'}{2J}\right). \tag{4}$$

With $J/k_B = 14.9$ K and $J'/k_B = 6.1$ K determined in the high-field ESR experiments [18], the gap for Cs_2CuBr_4 is estimated to be $\Delta = 0.84$ meV, which corresponds to 9.7 K or 203 GHz. This value perfectly agrees with our experimental observations. This agreement between the harmonic spin-wave theory for the exchange model and the experimental results might be somewhat fortuitous, as we completely neglected quantum fluctuations and the DM interactions. The observed agreement may indicate that these additional effects partially compensate each other[15].

The above consideration also predicts one more ESR mode arising from excitation of magnons with momenta $\mathbf{k} = \pm\mathbf{Q} + \mathbf{q}_b^* = (0,\ 2\pi/b \pm Q,\ 0)$ (M′ point in figure 6). The corresponding energy is

$$\Delta' = \epsilon_{\mathbf{q}_b^* \pm \mathbf{Q}} = 4J'S\left(1 - \frac{J'}{2J}\right)\sqrt{1 + \frac{J'}{J} + \frac{J'^2}{2J^2}}\,. \tag{5}$$

Using the above J and J' [18] we find $\Delta' \approx 1$ meV. As further calculations show, these excitations appear well inside the two-magnon continuum (figure 6), thus having a finite lifetime even at zero temperature. Therefore, they cannot be observed in ESR experiments. This conclusion is in agreement with the existing theoretical results for the damping of high-energy magnons in the spin-1/2 Heisenberg AF on a perfect triangular lattice [36–38].

For $H\|a$ and $H\|c$, two pairs of ESR modes were observed (A, A′, and C, C′, respectively); the corresponding frequency-field ESR diagrams and ESR spectra are shown in figure 7. The corresponding examples of ESR spectra are shown in figure 8 and figure 9. Upon rotating the sample around c- and a-axes, the modes A, A′ and C, C′ (respectively) merge into the single mode B at $H\|b$, which makes this direction special as it coincides with the direction of the order wavevector $\mathbf{Q}$. Noticeably, approaching the frequency 200 GHz, modes A′ and C became broader and weaker, so that no ESR was observed below 200 GHz.

It is important to mention, that due to the development of long-range 3D correlations below T_N one would expect the emergence of lower-frequency antiferromagnetic resonance (AFMR) magnon modes. Theory predicts the presence of at most three relativistic Goldstone AFMR modes as a consequence of the complete breaking of the rotational SO(3) symmetry in anisotropic spin systems with a noncollinear ground state [39]. Such AFMR modes have been recently observed in the isostructural compound Cs_2CuCl_4 below $T_N = 0.62$ K [40].

In conclusion, our work provides new insights into the unconventional spin dynamics in the spin-1/2 triangular-lattice antiferromagnet Cs_2CuBr_4, studied by means of high-field ESR spectroscopy. In particular, the temperature behavior of the observed zero-field energy gap is investigated in a broad temperature range, indicating that the gap is a characteristics of short-range-order spin correlations, which appear to persist in Cs_2CuBr_4 down to well below T_N. Based on the proposed spin-1/2 distorted triangle-lattice antiferromagnet

[15] Note, that the ratio $J/J' = 0.467$ determined for Cs_2CuBr_4 from the experimental value for the zero-field ordering wavevector $\mathbf{Q} = (0,\ 0.575,\ 0)$ [41, 42] using the classical expression is very close to $J/J' = 0.41\,(4)$ [18]. This suggests that effects of quantum fluctuations in Cs_2CuBr_4 may be significantly reduced (compared to the isostructural compound Cs_2CuCl_4).

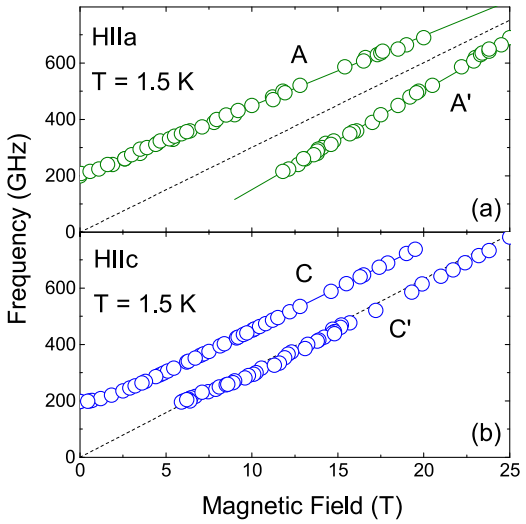

Figure 7. Frequency-field diagrams of ESR excitations with magnetic field applied along a (a) and c (b) axes. The dashed lines correspond to paramagnetic resonances with $g_a = 2.15$ ($H \| a, T = 77$ K) and $g_c = 2.26$ ($H \| c, T = 77$ K). Solid lines are guides for the eye. The data are obtained at 1.5 K.

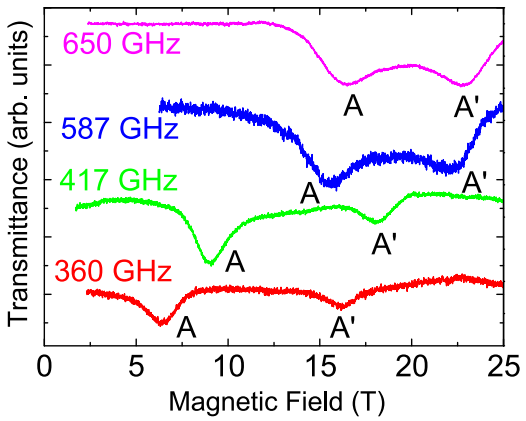

Figure 8. Examples of ESR spectra corresponding to the results shown in figure 7(a).

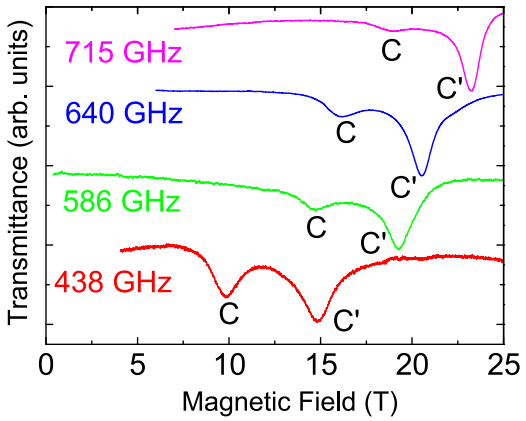

Figure 9. Examples of ESR spectra corresponding to the results shown in figure 7(b).

model, our findings might suggest, that Cs_2CuBr_4 exhibits a peculiar combination of nearly classical spin dynamics and static magnetic ordering (see footnote 13) with pronounced quantum effects as revealed, e.g., by the 1/3 magnetization plateau. This calls for further experimental quantification of the role of quantum fluctuations in Cs_2CuBr_4, in particular, for neutron measurements of the ordered magnetic moments and the magnon modes in zero magnetic field.

Acknowledgments

This work was supported by Deutsche Forschungsgemeinschaft (DFG, Germany). We acknowledge the support of the HLD at HZDR, member of the European Magnetic Field Laboratory (EMFL). A portion of this work was performed at the NHMFL, Tallahassee, FL, which is supported by NSF Cooperative Agreement No DMR-1157490, by the State of Florida, and by the DOE. S A Z appreciates the support of the Visiting Professor Program at Osaka University. Work at BNL was supported by the U S DOE under Contract No DE-AC02-98CH10886. C P acknowledges the support by the A von Humboldt Foundation. The authors would like to thank F H L Essler, V I Marchenko, O A Starykh, and A I Smirnov for fruitful discussions, M Ikeda and T Fujita for the help in high-field ESR experiments at AHMF, and S Miyasaka for his help orienting the samples.

References

[1] Anderson P W 1973 *Mater. Res. Bull.* **8** 153
[2] Bernu B, Lecheminant P, Lhuillier C and Pierre L 1994 *Phys. Rev.* B **50** 10048
[3] Capriotti L, Trumper A E and Sorella S 1999 *Phys. Rev. Lett.* **82** 3899
[4] Zheng W H, Fjaerestad J O, Singh R R P, McKenzie R H and Coldea R 2006 *Phys. Rev.* B **74** 224420
[5] White S R and Chernyshev A L 2007 *Phys. Rev. Lett.* **99** 127004
[6] Starykh O A and Balents L 2007 *Phys. Rev. Lett.* **98** 077205
[7] Ghamari S, Kallin C, Lee S S and Sørensen E S 2011 *Phys. Rev.* B **84** 174415
[8] Heidarian D, Sorella S and Becca F 2009 *Phys. Rev.* B **80** 012404
[9] Weng M Q, Sheng D N, Weng Z Y and Bursill R J 2006 *Phys. Rev.* B **74** 012407
[10] Weichselbaum A and White S R 2011 *Phys. Rev.* B **84** 245130
[11] Reuther J and Thomale R 2011 *Phys. Rev.* B **83** 024402
[12] Coldea R, Tennant D A, Tsvelik A M and Tylczynski Z 2001 *Phys. Rev. Lett.* **86** 1335
[13] Kohno M, Starykh O A and Balents L 2007 *Nat. Phys.* **3** 790
Kohno M 2009 *Phys. Rev. Lett.* **103** 197203
[14] Balents L 2010 *Nature* **464** 199
[15] Coldea R, Tennant D A, Cowley R A, McMorrow D F, Dorner B and Tylczynski Z 1996 *J. Phys.: Condens. Matter.* **8** 7473
[16] Povarov K Yu, Smirnov A I, Starykh O A, Petrov S V and Shipiro A Ya 2011 *Phys. Rev. Lett.* **107** 037204
[17] Morosin B and Lingafelter E C 1960 *Acta Crystallogr.* **13** 807
[18] Zvyagin S A *et al* 2014 *Phys. Rev. Lett.* **112** 077206
[19] Coldea R, Tennant D A, Habicht K, Smeibidl P, Wolters C and Tylczynski Z 2002 *Phys. Rev. Lett.* **88** 137203
[20] Radu T, Wilhelm H, Yushankhai V, Kovrizhin D, Coldea R, Tylczynski Z, Luhmann T and Steglich F 2005 *Phys. Rev. Lett.* **95** 127202
[21] Fortune N A, Hannahs S T, Yoshida Y, Sherline T E, Ono T, Tanaka H and Takano Y 2009 *Phys. Rev. Lett.* **102** 257201
[22] Ono T *et al* 2005 *Progr. Theor. Phys. Suppl.* **159** 217
[23] Zvyagin S A, Krzystek J, van Loosdrecht P H M, Dhalenne G and Revcolevschi A 2004 *Physica* B **346-347** 1
[24] Zaliznyak I A, Lee S-H and Petrov S V 2001 *Phys. Rev. Lett.* **87** 017202
[25] Coldea R, Tennant D A and Tylczynski Z 2003 *Phys. Rev.* B **68** 134424
[26] Lake B, Tennant D A and Nagler S E 2000 *Phys. Rev. Lett.* **85** 832
Lake B, Tennant D A and Nagler S E 2005 *Phys. Rev.* B **71** 134412
[27] Lake B, Tennant D A, Frost C D and Nagler S N 2005 *Nature* **4** 329
[28] Tanaka H, Ono T, Katori H A, Mitamura H, Ishikawa F and Goto T 2002 *Prog. Theor. Phys. Suppl.* **145** 101
[29] Veillette M Y, James A J A and Essler F H L 2005 *Phys. Rev.* B **72** 134429
[30] Dalidovich D, Sknepnek R, Berlinsky A J, Zhang J and Kallin C 2006 *Phys. Rev.* B **73** 184403
[31] Brill T M, Boucher J P, Voiron J, Dhalenne G, Revcolevschi A and Renard J P 1994 *Phys. Rev. Lett.* **73** 1545
[32] Sieling M, Löw U, Wolf B, Schmidt S, Zvyagin S and Lüthi B 2000 *Phys. Rev.* B **61** 88
[33] Kamenskyi D, Wosnitza J, Krzystek J, Aczel A A, Dabkowska H A, Dabkowski A B, Luke G M and Zvyagin S A 2013 *J. Low Temp. Phys.* **170** 231
[34] Wang Z *et al* 2014 *Phys. Rev.* B **89** 174406
[35] Sakai T, Cepas O, Ziman T and Phys J 2000 *Soc. Japan.* **69** 3521
[36] Zhitomirsky M E and Chernyshev A L 2013 *Rev. Mod. Phys.* **85** 219
[37] Chernyshev A L and Zhitomirsky M E 2009 *Phys. Rev.* B **79** 144416
[38] Mourigal M, Fuhrman W T, Chernyshev A L and Zhitomirsky M E 2013 *Phys. Rev.* B **88** 094407
[39] Andreev A F and Marchenko V I 1976 *Zh. Eksp. Teor. Fiz.* **70** 1522
Andreev A F and Marchenko V I 1976 *Sov. Phys.—JETP* **43** 794
[40] Smirnov A I, Povarov Yu K, Petrov S V and Shapiro Ya A 2012 *Phys. Rev.* B **85** 184423
[41] Ono T *et al* 2004 *J. Phys.: Condens. Matter.* **16** S773
[42] Ono T, Tanaka H, Aruga Katori H, Ishikawa F, Mitamura H and Goto T 2003 *Phys. Rev.* B **67** 104431